HHS Public Access

Author manuscript

Biol Psychiatry. Author manuscript; available in PMC 2019 December 01.

Published in final edited form as:

Biol Psychiatry. 2018 December 01; 84(11): 817–826. doi:10.1016/j.biopsych.2017.06.022.

Altered GluA1 function and accumbal synaptic plasticity in the *Clock*Δ19 model of bipolar mania

Puja K. Parekh, BS[1], **Darius Becker-Krail, BS**[1], **Poornima Sundaravelu**[1], **Shinsuke Ishigaki, PhD**[2], **Haruo Okado, PhD**[3], **Gen Sobue, PhD**[2], **Yanhua Huang, PhD**[1], and **Colleen A. McClung, PhD**[1]

[1]University of Pittsburgh Medical Center, Department of Psychiatry, Pittsburgh, Pennsylvania 15219

[2]Department of Neurology, Nagoya University Graduate School of Medicine, Nagoya 466-8550, Japan

[3]Department of Brain Development and Neural Regeneration, Tokyo Metropolitan Institute of Medical Science, Tokyo 156-8506, Japan

Abstract

Background—Disruptions in circadian rhythms are associated with an increased risk for bipolar disorder (BD). Moreover, studies show that the circadian protein CLOCK is involved in regulating monoaminergic systems and mood-related behavior. However the molecular and synaptic mechanisms underlying this relationship remain poorly understood.

Methods—Using *ex vivo* whole cell patch clamp electrophysiology in *Clock*Δ19 mutant and wildtype (WT) mice we characterized alterations in excitatory synaptic transmission, strength and intrinsic excitability of nucleus accumbens (NAc) neurons. We performed protein crosslinking and Western blot analysis to examine surface and intracellular levels and rhythm of the glutamate receptor subunit, GLUA1, in the NAc. Viral-mediated overexpression of *GluA1* in the NAc and behavioral assays were also used.

Results—Compared with WT mice, *Clock*Δ19 mice display reduced AMPAR-mediated excitatory synaptic responses at NAc medium spiny neurons (MSNs). These alterations are likely postsynaptic as presynaptic release of glutamate onto MSNs is unaltered in mutants. Additionally, NAc surface protein levels and the rhythm of GLUA1 are decreased in *Clock*Δ19 mice diurnally, consistent with reduced functional synaptic response. Furthermore, we observed a significantly hyperpolarized resting membrane potential of *Clock*Δ19 MSNs suggesting lowered intrinsic excitability. Lastly, overexpression of functional *GluA1* in the NAc of mutants was able to

Corresponding Author: Colleen A. McClung, PhD, University of Pittsburgh Medical Center, 450 Technology Dr. Suite 223, Pittsburgh, Pennsylvania 15219, Office (412)624-5559, Fax (412), mcclungca@upmc.edu.

Financial disclosures

The authors report no biomedical financial interests or potential conflicts of interest.

normalize increased exploratory drive and reward sensitivity behavior when mice are in a manic-like state.

Conclusions—Together, our findings demonstrate that NAc excitatory signaling via GLUA1 expression is integral to the effects of *Clock* gene disruption on “manic-like” behaviors.

Keywords

Circadian; CLOCK; Nucleus Accumbens; Glutamatergic; Excitability; Mania

Introduction

Endogenously generated circadian rhythms allow organisms to adaptively entrain to life on earth by coordinating behavior with photic and non-photic environmental cues (1). The suprachiasmatic nucleus (SCN) synchronizes subsidiary clocks throughout the brain and periphery, however local, SCN-autonomous molecular rhythms can be found. Cells orchestrate molecular rhythms through a series of transcriptional-translational feedback loops (2; 3). Genome-wide studies suggest that variations in clock genes are strongly associated with human neuropsychiatric illnesses including substance abuse disorders and bipolar disorder (BD), a highly disruptive condition affecting 1–3% of the U.S. population (4–7). BD is characterized by mood cycling through manic, depressive and euthymic states (8). A complex bidirectional relationship exists between circadian disruption and BD whereby polymorphisms in circadian genes confer risk for the disease in predisposed individuals and those suffering from it often experience abnormal rhythms (9). Recently, BD has been re-conceptualized by some as a synaptic disorder where the functions of postsynaptic proteins are altered in prefrontal and striatal regions, potentially producing circuit-level consequences affecting normal mood and reward response (10; 11). Additionally, mood-stabilizing agents exert their effects in part by acting directly on synaptic elements including glutamatergic transmission (11; 12).

Our lab and others have previously characterized a “manic-like” behavioral profile in mice harboring a point mutation in the 19th exon of the *Clock* gene, producing a dominant negative CLOCK protein capable of DNA binding but deficient in transcriptional activity (13; 14). These *Clock*Δ19 mice display hyperactivity, increased exploratory drive, lowered depression-like behavior, reduced sleep, greater impulsivity and increased reward response (15–20). Moreover, *Clock*Δ19 mice are hyperdopaminergic, with elevated ventral tegmental area (VTA) dopamine neuron activity and dopamine signaling in the nucleus accumbens (NAc) (17; 21; 22). The NAc consists primarily of GABAergic medium spiny neurons (MSNs) and integrates limbic and motor information to drive motivated behavior. Afferent glutamatergic inputs to the nucleus originate mainly from the prefrontal cortex, hippocampus and amygdala as well as a prominent dopaminergic projection from the VTA (23). Dopamine reliably modulates the activity of glutamate at MSN synapses via second messenger signaling, having implications for substance abuse and mood disorders (24–26). Furthermore, imaging studies of un-medicated BD patients indicate significantly lower striatal dopamine transporter (DAT) availability suggesting abnormal dopamine transmission and reward processing in this region (27).

The consequences of *Clock* disruption on network activity in mesocorticolimbic circuitry have been investigated in greater depth. We previously reported reduced total NAc protein levels of the α-amino-3-hydroxy-5-methyl-4-isoxazolepropionic acid (AMPA) type glutamate receptor subunit, GLUA1, and phosphorylated GLUA1 (P-GLUA1 Ser^{845}) as well as altered MSN dendritic morphology in *Clock*Δ19 mice. Furthermore, mutants exhibit diminished cross-frequency phase coupling of neural oscillations within the NAc and coherence with cortico-limbic regions during exploration of a novel environment (28). NAc phase coupling depends upon glutamatergic signaling and computational models suggest that altered AMPAR and NMDAR function can shift synaptic weights, disrupting the ability of MSNs to entrain to afferent input (29). It has been proposed that this imbalance within accumbal circuitry can alter functioning of downstream target regions within networks regulating goal-directed behavior (28). Given the increased dopaminergic tone of *Clock*Δ19 mice, we hypothesized that there may be adaptations in NAc microcircuitry indicative of plasticity.

Here we sought to investigate the effects of *Clock*Δ19 on excitatory drive onto NAc MSNs as well as the expression and rhythm of accumbal GLUA1 protein and intrinsic excitability of MSNs. While rhythms in dopamine, glutamate and GABA neurotransmission have been demonstrated in the accumbens (30), *ex vivo* electrophysiological studies of diurnal activity in excitatory synaptic function have been lacking. We therefore conducted our physiological and biochemical measures across the light/dark cycle. Additionally, we examined whether manipulation of *GluA1* in the NAc could normalize aspects of the “manic-like” behavioral profile in *Clock*Δ19 mice.

Materials and Methods

Animals

*Clock*Δ19 mice were created by *N*-ethyl-*N*-nitrosurea (ENU) mutagenesis (13). Mutant (*Clock*/*Clock*) and wildtype (+/+) littermates (BALB/cJ and C57BL/6J mixed background) were bred from heterozygote (*Clock*Δ19/+) pairs and group housed. Animals used in this study were maintained on a BALB/cJ background. Male and female mutant and WT mice (6–9wks) were used for electrophysiological experiments. Hyperactivity in response to novelty, a key manic-like feature of *Clock*Δ19 mice was apparent within this age range ($t_{(10)}$=5.376, P=0.0003) (fig.S1). Male mice (8–12wks) were used for biochemical and behavioral experiments. Mice were maintained on a 12:12h light/dark cycle (ZT 0 = lights on 7:00AM; ZT 12 = lights off 7:00PM) or a reverse 12h light cycle. For 24hr time-series experiments, mice were group housed in temperature-controlled, soundproof cabinets with light cycles precisely regulated. Food and water were available *ad libitum*. All animal use was conducted in accordance with the National Institute of Health guidelines for the care and use of laboratory animals and approved by the Institutional Animal Care and Use Committee of the University of Pittsburgh.

NAc slice preparation

Animals were rapidly anesthetized with isoflurane and decapitated. Brains were removed into ice-cold oxygenated (95% O_2/5% CO_2) modified aCSF containing (in mM): 135 *N*-

methyl-D-glucamine, 1 KCl, 1.2 KH_2PO_4, 1.5 $MgCl_2$, 0.5 $CaCl_2$, 70 choline bicarbonate, and 10 D-glucose; pH 7.4 adjusted with HCL. NAc-containing coronal slices (200mm) were sectioned with a vibratome (VT1200S; Leica, Wetzlar, Germany) and incubated for 30 minutes at 37°C in oxygenated aCSF containing (in mM): 119 NaCl, 26 $NaHCO_3$, 2.5 KCl, 1 NaH_2PO_4, 2.5 $CaCl_2$, 1.3 $MgCl_2$, 11 D-glucose. Slices were kept in room temperature aCSF until recording (30–32°C).

Whole-cell patch-clamp recordings

Slices were viewed by differential interference contrast (DIC) optics (Leica) and the accumbens was localized under low magnification. Recordings were made under visual guidance with 40x objective. Cells were voltage clamped at −70mV. pClamp10 software (Molecular Devices, Sunnyvale, CA) was used to analyzed data. For mEPSC analysis, 250–2500 events were collected. AMPA/NMDA ratios were determined by taking the average peak amplitude of EPSCs at 40mV in the absence or presence of D-APV (30 sweeps) or at −70mV. For paired pulse experiments, a set of two pulses was delivered (every 10s) with varying inter-pulse intervals (30 sweeps). Decay kinetics were measured automatically and CV was calculated as the standard deviation over mean of individual EPSC amplitudes (30 sweeps). For current clamp, membrane potential was adjusted to −80mV with minimal current injection. A current step protocol from −200pA to 400pA was applied (50pA increment; 5 runs). Details are provided in supplementary methods.

Surface GLUA1 detection

Slight modifications were made to a previously described protocol (31). Briefly, NAc tissue was removed for crosslinking with the BS^3 reagent (Pierce, Waltham, MA). Crosslinked and non-crosslinked protein samples were processed with immunoblotting to determine GLUA1 membrane and intracellular protein levels. Details are provided in supplementary methods.

Viral gene transfer and stereotaxic surgery

Stereotaxic surgery was performed as previously described (32). Purified high titer AAV9 encoding *GluA1* driven by the human synapsin promoter or AAV9-hsyn-GFP (0.5μL) (33) was bilaterally injected into the NAc. *GluA1* overexpression was confirmed by real-time RT-PCR from infected NAc tissue as described in the supplement. Mice recovered for 3 weeks allowing for full viral expression. Viral placements were verified using immunohistochemical methods as described in the supplement. Use of AAV-*Clock*-shRNA virus has been previously reported (34). Injections were made in 5–6wk old animals.

Animal behavior

Animals habituated to testing rooms for at least 30 minutes. Testing occurred early in the light phase (ZT0-ZT4) or dark phase (ZT12–16). Assay details are provided in the supplementary methods.

Data analysis

Electrophysiological, biochemical and behavioral experiments were conducted blind to genotype. Significant differences were determined by Student's *t*-Test, one-way-or two-way

ANOVA followed by Bonferroni *post hoc* tests. $P<0.05$ is considered significant for all analyses. All data are presented as mean ± SEM.

Results

*Clock*Δ19 mice have reduced AMPAR-mediated synaptic transmission and strength at NAc MSNs

We observed a significant reduction in glutamatergic synaptic transmission in *Clock* mutant MSNs compared with WT across the L/D cycle as indicated by reduced amplitude of AMPAR-mediated miniature excitatory postsynaptic currents (mEPSCs) ($F_{(1,76)}=16.43$, $P=0.0001$ genotype effect). A significant effect of phase in mEPSC amplitude was found as well suggesting that perhaps this particular measure has diurnal variability ($F_{(1,76)}=6.615$, $P=0.0121$ phase effect) (fig.1c). Studies have shown that signaling in core and shell sub-regions of the NAc can mediate affective valence and motivational behavior in a distinct manner (35; 36). However, when we further analyzed mEPSC amplitude in NAc core versus shell neurons, no significant difference was observed during the light ($F_{(1,37)}=9.205$, $P=0.0044$ genotype effect; $F_{(1,37)}=0.0001$, $P=0.9910$ region effect) or dark phase ($F_{(1,34)}=6.715$, $P=0.0140$ genotype effect; $F_{(1,34)}=0.0491$, $P=0.8259$ sub-region effect) (fig. S2a–b). When calculating AMPAR/NMDAR ratio of evoked EPSCs, a measure of excitatory synaptic strength, we detected a significant reduction in A/N of MSNs in *Clock*Δ19 mutants (~30% decrease in AMPAR EPSC amplitude and minimal change in NMDAR current), particularly within the light phase ($F_{(1,44)}=11.53$, $P=0.0015$ genotype effect; $F_{(1,44)}=0.1237$, $P=0.7267$ phase effect) (fig.1f) and no change in the decay kinetics of the NMDA current indicating that subunit stoichiometry of these receptors was not altered in mutants ($F_{(1,39)}=0.1936$, $P=0.6624$ genotype effect; $F_{(1,39)}=2.013$, $P=0.1639$ phase effect) (fig.S3b). Additionally, we failed to observe an effect of genotype or phase on the CV analysis of NMDAR EPSCs relative to AMPAR EPSCs, a measure directly correlated with the proportion of silent synapses, which lack functional AMPARs ($F_{(1,29)}=0.0944$, $P=0.7609$ genotype effect; $F_{(1,29)}=0.4760$, $P=0.4957$ phase effect) (fig.S3d). This result indicates that the reduced functionality of AMPAR-mediated activity at mutant MSNs likely does not occur through a complete silencing of synapses.

Presynaptic release of glutamate onto NAc MSNs is unaltered in *Clock* mutants

We further analyzed the frequency of mEPSCs as a measure of quantal release probability of glutamate at MSNs in mutant and WT slices. Here, we found no significant difference between groups or by diurnal phase ($F_{(1,72)}=0.06752$, $P=0.7957$ genotype effect; $F_{(1,\ 72)}=0.04288$, $P=0.8365$) (fig.2a). Another standard measure of transmitter release probability at excitatory synapses is the paired pulse ratio (PPR) comprised of the peak amplitude of the 2nd of a series of evoked EPSCs to the 1st. The PPR is inversely related to release probability. We determined the PPR at three different inter-pulse intervals and observed no significant difference between mutant and WT groups during either diurnal phase ($F_{(3,\ 25)}=0.1803$, $P=0.9088$ genotype effect; $F_{(3,\ 25)}=9.531$, $P=0.0003$ interval effect) (fig.2d). Together these results suggest that synapse number or presynaptic release of glutamate onto MSNs remain unchanged with *Clock* gene disruption and wildtype animals do not show diurnal variability in these measures.

Membrane levels and rhythm of GLUA1 protein are reduced in the NAc of *Clock*Δ19 mice

In order to investigate the molecular basis for the diminished excitatory drive seen in *Clock* mutant NAc, we measured the diurnal protein expression of the AMPAR subunit, GLUA1. Previously, we have shown reduced total and phosphorylated protein levels of this particular subunit in mutant NAc during the day (28) suggesting a potential deficiency in the translation or trafficking of AMPARs that may underlie microcircuit-level and physiological dysfunction. Here we used BS^3 crosslinking to isolate membrane-bound and intracellular fractions of GLUA1. The inherent smearing of crosslinking to detect multi-protein complexes made it difficult to resolve a clear multimer band and we therefore quantified the reduction of the monomer to determine the amount of surface expressed GLUA1. We found a significant reduction in the surface/intracellular (S/I) ratio of GLUA1 normalized to GAPDH at ZT6 and ZT18 in mutant NAc which overlapped with our recording times ($F_{(1, 20)}$=17.67, P=0.0004 genotype effect; $F_{(1, 20)}$=0.8999, P=0.3541 phase effect) (fig.3). These results suggest that reduction in CLOCK protein function may affect the ability of GLUA1-containing AMPARs to be inserted into the membrane for proper excitatory signaling and this deficit appears across time of day. Furthermore, we tested for a rhythm in GLUA1 total protein and S/I ratio in WT and mutant NAc. Using multiple harmonic regression, we detected a significant diurnal rhythm in WT GLUA1, with a bimodal pattern peaking at the midpoints of the light and dark cycles (P<0.0001). A similar rhythm was also detected in the S/I ratio in WT NAc (P<0.001). In mutant accumbens however, we were unable to fit the total and surface GLUA1 data indicating a lack of significant rhythm (fig. 4a–b). Additionally, when we analyzed whether *Clock* mutants have a shift in the expression pattern of GLUA1, we found that indeed the acrophase, or estimation of circadian phase corresponding to the peak of the rhythm, was significantly advanced in mutants for both the total protein and S/I ratio (P<0.05) (fig.4c). We therefore conclude that a biochemical basis contributing to excitatory drive onto MSNs is profoundly affected by a lack of proper CLOCK protein function.

Clock mutant MSNs display subtle alterations in intrinsic membrane properties

The functional output of MSNs depends upon the integration of synaptic inputs and the inherent membrane excitability. In order to assess the effects of the *Clock*Δ19 mutation on MSN functional output, we first measured the evoked firing rate of MSNs in response to increasing current injection. While we did not observe a significant difference in spiking between genotypes, interestingly, we saw a robust difference in excitability by phase with a highly increased firing rate during the dark cycle (fig.5b). When collapsing across genotype we detected significant differences by phase and current injection ($F_{(3, 39)}$=48.87, P<0.0001 phase effect; $F_{(6, 234)}$=699.8, P<0.0001 current effect) (fig.5b). Relatively few *ex vivo* studies have measured diurnal neuronal activity in extra-SCN regions; therefore, the variable intrinsic excitability profile of NAc MSNs is noteworthy. A number of potential mechanisms could underlie this, including Clock-regulated fluctuations in the activity of potassium conductances responsible for MSN bi-stable excitability (37–39). We further analyzed active and passive intrinsic membrane properties of mutant and WT MSNs across the light/dark cycle, including the resting membrane potential (RMP), the rheobase or minimum current needed for action potential (AP) generation, the AP threshold and input resistance (R_i) at −50pA (summarized in Table 1). We observed a significantly lower RMP of *Clock* mutant

MSNs compared with WT during both phases, suggesting that mutant MSNs may rest at a more hyperpolarized membrane potential at baseline and require greater stimulation to enter the “up-state”. We did not find a significant difference in the rheobase during either phase. AP threshold was similar during the light phase, however was lower in mutant MSNs in the dark. Lastly, R_i did not differ significantly by genotype in either phase, however was higher during the dark phase in both groups, which may account in part for the increased firing rate. Overall, we find that a reduction in CLOCK protein function does not affect the intrinsic membrane excitability of MSNs, however a lowered resting membrane potential may indicate a more subtle effect on excitability.

Overexpression of *GluA1* in the NAc normalizes “manic-like” behavior in *Clock*Δ19 mice

Finally, we sought to determine whether up-regulation of functional *GluA1* expression in *Clock*Δ19 NAc could rescue their abnormal exploratory drive and reward sensitivity. We have reported previously that *Clock* mutants display mood cycling with manic-like behavior during the day and euthymic behavior at night (40). Here we injected AAV9-hsyn-*GluA1* or AAV9-hsyn-GFP bilaterally into the accumbens of adult male mutant and WT mice. Neuronal expression was confirmed with NeuN staining (fig.S4). Our manipulation resulted in a significant increase in *GluA1* mRNA ($t_{(7)}$=2.664, P=0.0323) (fig.6a–c) and a potentiation of excitatory synapses in mutant ($t_{(12)}$=3.608, P=0.0036) (fig.S5a–b) and WT MSNs ($t_{(11)}$=3.429, P=0.0056) (fig.S5c–d). In the light phase, similar to lithium treatment, (16) overexpression of *GluA1* in *Clock* mutants did not alter the failure to habituate to a novel environment that was seen in GFP-expressing mutant mice. As expected, WT control groups showed faster locomotor habituation in this assay ($F_{(17, 816)}$=83.17, P<0.0001 time effect; $F_{(3, 48)}$=3.522, P<0.0218 genotype effect) (fig.6d). In a measure of exploratory drive behavior, total time spent in the open arms of the elevated plus maze (EPM) was decreased to near WT levels with *GluA1* up-regulation in mutant NAc ($F_{(1, 54)}$=1.498, P=0.2262 treatment effect; $F_{(1, 54)}$=7.989, P=0.0066 interaction; Bonferroni’s test: **P<0.01, ***P<0.001) (fig.6e). As expected, GFP expressing mutant mice displayed increased open arm time compared with WT ($F_{(1, 54)}$=8.057, P=0.0064 genotype effect) (fig.6e). Comparable to previous studies, mutant mice expressing GFP had a significantly higher proportion of open arm entries (normalized to total crosses) compared with WT GFP-expressing mice ($F_{(1, 54)}$=6.427, P=0.0142 genotype effect) and similar to lithium treatment, several weeks of NAc-specific *GluA1* overexpression in mutants resulted in a significant reduction in open arm entries compared with GFP expression ($F_{(1, 54)}$=0.9928, P=0.3235 treatment effect; $F_{(1, 54)}$=6.009, P=0.0175 interaction; Bonferroni’s test: *P<0.05, ***P<0.001) (fig.6f). To determine whether GLUA1-mediated signaling is important for the effects of *Clock* gene disruption on behavioral measures associated with cocaine reward sensitivity, we performed cocaine conditioned place preference (CPP). Using a dose of 5mg/kg cocaine, which has been shown to increase preference in *Clock* mutant mice compared with WT littermates (17), we found a reliably elevated CPP score in GFP-expressing mutants compared with WT ($F_{(1, 53)}$=2.514, P=0.1188 genotype effect; $F_{(1, 53)}$=1.817, P=0.1834 treatment effect; $F_{(1, 53)}$=22.78, P<0.0001 interaction; Bonferroni’s test: *P<0.05, ***P<0.001) (fig.6g). *GluA1* overexpression in *Clock* mutants was able to normalize CPP to WT levels. Unexpectedly, we also observed a marked increase in place preference in WT mice with *GluA1* up-regulation. During the dark phase, in contrast, *GluA1*

overexpression did not alter locomotor activity ($F_{(17, 648)}$=17.82, P<0.0001 time effect; $F_{(3, 648)}$=100.7, P<0.0001 genotype effect) (fig.S6a), EPM open arm time ($F_{(1, 35)}$=3.335, P=0.0764 genotype effect; $F_{(1, 35)}$=0.6103, P=0.4399 treatment effect; $F_{(1, 35)}$=0.8201, P=0.3714 interaction) (fig.S6b), or open arm entries ($F_{(1, 35)}$=4.712, P=0.0368 genotype effect; $F_{(1, 35)}$=0.7050, P=0.4068 treatment effect; $F_{(1,35)}$=0.7643, P=0.3880 interaction) (fig6c). These results are in keeping with the previously reported euthymic behavior of mutants during this phase (40). When we examined the effect of overexpression on cocaine CPP, we also found no significant effects of viral expression ($F_{(1,36)}$=3.591, P=0.0662 genotype effect; $F_{(1,36)}$=0.4940, P=0.4867 treatment effect; $F_{(1, 36)}$=1.225, P=0.2757 interaction) (fig.S6d). This is the first examination of cocaine preference in mutant and WT animals during the active phase and interestingly, the CPP score of GFP-expressing WT animals is elevated compared with the inactive phase. We have previously described a rhythm in the expression of tyrosine hydroxylase in WT animals with a peak during the dark cycle (40). This could underlie the diurnal variance in reward response.

Discussion

The current study demonstrates that CLOCK disruption produces significantly reduced excitatory drive onto accumbal medium spiny neurons. We found that both the amplitude of mutant AMPAR-mediated spontaneous currents as well as the AMPAR/NMDAR ratio of evoked currents was decreased and this does not appear to occur through silent synapse generation. Furthermore, these adaptations are likely postsynaptic as presynaptic release probability remained unchanged. Additionally, *Clock* mutation dampened a normal bimodal rhythm in GLUA1 protein expression and advanced the acrophase. In a previous study we reported a significant decrease in both total and phosphorylated GLUA1 protein levels in mutant NAc during the day with no changes in GLUA2, GLUN1, GLUN2A or GLUN2B subunit expression (28). These results suggested a potential deficit in the translation or trafficking of GLUA1-containing AMPARs to NAc synapses. Here we demonstrate that indeed, membrane-bound GLUA1 levels are lowered with *Clock* mutation across light and dark phases. Therefore, functional impairments in glutamatergic transmission and strength of mutant MSNs may result from reduced synaptic GLUA1-containing AMPARs. Increased activity of VTA dopamine neurons and elevated extracellular dopamine levels are likely an indirect cause for these abnormalities in *Clock*Δ19 MSNs. The modulatory function of dopamine on NAc glutamatergic activity is characterized in studies in which drugs of abuse act to elevate dopamine levels. Chronic cocaine administration, for instance, leads to an up-regulation of surface-expressed GLUA1 (41–43). Importantly, chronic-cocaine induced plastic changes are not recapitulated in this model of hyperdopaminergia, implying that the observed effects are likely a compensatory response to a state of continually elevated dopaminergic activity. Additionally, the manner in which cocaine and dopamine influence synaptic and intrinsic properties of MSNs through differential signaling mechanisms has been empirically and theoretically examined (44; 45). Modulatory effects of dopamine on MSNs are thought to differ based upon the specific dopamine receptor expression. One limitation of our study is the inability to determine the cellular identity of MSNs in *Clock* mutant slices. We have previously reported an imbalance in D1R and D2R–mediated signaling in the striatum of mutants whereby there is a shift towards increased expression

and binding activity of D2Rs (21). Therefore, it is possible that these changes are predominant within particular pathways (i.e. “direct” versus “indirect”). When we investigated the intrinsic excitability of mutant and WT MSNs we observed similar firing however MSN excitability was significantly elevated during the dark phase. Rhythmicity in a number of ionic mechanisms could underlie this interesting effect. For instance, diurnal variations in resting membrane potential, calcium currents, potassium conductances and *in vitro* firing patterns have been reported in midline thalamic neurons. Activity of these neurons is also elevated during the dark phase (46).

As a critical site for integration of limbic and sensorimotor information, the accumbens is important for maintaining proper mood and reward responses. *Clock*Δ19 mice display heightened exploratory behavior and robustly elevated sensitivity to a variety of rewarding substances. While *Clock*Δ19 mice also show reduced sensorimotor gating similar to BD manic patients, the pattern of locomotor activity during exploration is not replicated, suggesting that, as with all animal models, limitations exist (20). However, similar to BD patients, *Clock* mutant mice also show precipitations in manic-like episodes when their sleep cycle is disrupted (during the light) (47–49), mirroring what occurs in human subjects, thus they can help elucidate the biological mechanisms that lead to manic behavior induced by sleep/wake cycle disruption. Furthermore, restoration of functional CLOCK in the VTA and treatment with dopamine depleting pharmacological agents are able to normalize many aspects of the mutant manic-like phenotype (16; 40). Disruption of glutamate receptor expression in the striatum has also been linked with neuropsychiatric illness and increased dopaminergic transmission. Wiedholz and colleagues characterized a number of schizophrenia-relevant impairments in *GluA1* knock-out mice including hyperactivity and reduced striatal clearance of extracellular dopamine (50). Other preclinical models characterized by glutamatergic dysfunction have been likened to features of BD including *GluN2A* deletion and *GluR6* subunit knock-out (51; 52). Here, we have demonstrated that restoring functional expression of GLUA1-containing AMPARs to the accumbens is sufficient to normalize exploratory behavior in *Clock* mutants. Future studies may determine whether GLUA1 overexpression normalizes mutant accumbal phase signaling deficits as well. Up-regulation of GLUA1 in the NAc also reduced cocaine place preference in mutants. Interestingly, we observed robust increase in preference in WT animals in which GLUA1 was overexpressed. This was surprising given that Bachtell and colleagues have demonstrated decreased sensitization and cocaine seeking (extinction and reinstatement) following overexpression of *GluA1* in the NAc in rats (53). However, the specific mode of up-regulation in these studies varied from our own, in which long-term overexpression may have altered accumbal network activity in a more pronounced manner. Additionally, while the level of synaptic potentiation induced by our viral overexpression was similar in WT and mutant MSNs, the difference in CPP could depend upon the type of AMPARs inserted (calcium permeable or impermeable).

Interestingly, the physiological, behavioral and biochemical changes that we describe in *Clock* mutants are unlikely due to direct transcriptional mechanisms in the accumbens but rather may be tied to dysfunctional circuit dynamics. We have previously reported that a viral-mediated knock-down of CLOCK in the NAc does not alter cocaine CPP (32) and we find here that it does not affect the amplitude and frequency of MSN mEPSCs

($F_{(2, 53)}$=4.545, P=0.0151 treatment effect) (fig.S7). While the amplitude of mEPSCs, GLUA1 expression and RMP are consistently decreased in mutants across the L/D cycle, the AMPAR/NMDAR ratio is only altered during the light and *GluA1* overexpression only normalizes behavior in the animals' inactive phase when it is significantly disrupted compared to WT. Collectively, these results support a hypothesis whereby diminished CLOCK function increases dopaminergic activity and tone, altering excitatory drive onto MSNs. This may reduce the functional output of the accumbens in feedback dynamics onto the VTA or disinhibit other target regions leading to the elevation of mood, exploratory drive and reward-seeking behavior, however this would have to be directly investigated in future studies.

Supplementary Material

Refer to Web version on PubMed Central for supplementary material.

Acknowledgments

We thank Mark Brown, Mariah Hildebrand, Heather Buresch and Emily Webster, for expert animal care and husbandry and technical assistance. We also thank Dr. Marina Wolf and Dr. Oliver Schluter for methodological advice and Dr. Ryan Logan for editorial comments. This work was supported by NIH T32 DA03111 (PKP), NIH MH082876, DA023988 (CAM), IMHRO, The McKnight Foundation, and the Brain and Behavior Foundation (NARSAD) (CAM).

References

1. Reppert SM, Weaver DR. Coordination of circadian timing in mammals. Nature. 2002; 418:935–41. [PubMed: 12198538]
2. Ko CH, Takahashi JS. Molecular components of the mammalian circadian clock. Hum Mol Genet 15 Spec No. 2006; 2:R271–7.
3. Lowrey PL, Takahashi JS. Genetics of circadian rhythms in Mammalian model organisms. Adv Genet. 2011; 74:175–230. [PubMed: 21924978]
4. McClung CA. Circadian genes, rhythms and the biology of mood disorders. Pharmacol Ther. 2007; 114:222–32. [PubMed: 17395264]
5. Soria V, Martínez-Amorós E, Escaramís G, Valero J, Pérez-Egea R, García C, et al. Differential association of circadian genes with mood disorders: CRY1 and NPAS2 are associated with unipolar major depression and CLOCK and VIP with bipolar disorder. Neuropsychopharmacology. 2010; 35:1279–89. [PubMed: 20072116]
6. McCarthy MJ, Welsh DK. Cellular circadian clocks in mood disorders. J Biol Rhythms. 2012; 27:339–52. [PubMed: 23010657]
7. Logan RW, Williams WP, McClung CA. Circadian rhythms and addiction: mechanistic insights and future directions. Behav Neurosci. 2014; 128:387–412. [PubMed: 24731209]
8. Miklowitz DJ, Johnson SL. The psychopathology and treatment of bipolar disorder. Annu Rev Clin Psychol. 2006; 2:199–235. [PubMed: 17716069]
9. McClung CA. How might circadian rhythms control mood? Let me count the ways. Biol Psychiatry. 2013; 74:242–9. [PubMed: 23558300]
10. Meador-Woodruff JH, Hogg AJ, Smith RE. Striatal ionotropic glutamate receptor expression in schizophrenia, bipolar disorder, and major depressive disorder. Brain Res Bull. 2001; 55:631–40. [PubMed: 11576760]
11. De Bartolomeis A, Buonaguro EF, Iasevoli F, Tomasetti C. The emerging role of dopamine-glutamate interaction and of the postsynaptic density in bipolar disorder pathophysiology: Implications for treatment. J Psychopharmacol (Oxford). 2014; 28:505–526. [PubMed: 24554693]

12. Du J, Gray NA, Falke CA, Chen W, Yuan P, Szabo ST, et al. Modulation of synaptic plasticity by antimanic agents: the role of AMPA glutamate receptor subunit 1 synaptic expression. J Neurosci. 2004; 24:6578–89. [PubMed: 15269270]
13. King DP, Zhao Y, Sangoram AM, Wilsbacher LD, Tanaka M, Antoch MP, et al. Positional cloning of the mouse circadian clock gene. Cell. 1997; 89:641–53. [PubMed: 9160755]
14. Gekakis N, Staknis D, Nguyen HB, Davis FC, Wilsbacher LD, King DP, et al. Role of the CLOCK protein in the mammalian circadian mechanism. Science. 1998; 280:1564–9. [PubMed: 9616112]
15. Easton A, Arbuzova J, Turek FW. The circadian Clock mutation increases exploratory activity and escape-seeking behavior. Genes Brain Behav. 2003; 2:11–9. [PubMed: 12882315]
16. Roybal K, Theobold D, Graham A, DiNieri JA, Russo SJ, Krishnan V, et al. Mania-like behavior induced by disruption of CLOCK. Proc Natl Acad Sci USA. 2007; 104:6406–11. [PubMed: 17379666]
17. McClung CA, Sidiropoulou K, Vitaterna M, Takahashi JS, White FJ, Cooper DC, Nestler EJ. Regulation of dopaminergic transmission and cocaine reward by the Clock gene. Proc Natl Acad Sci USA. 2005; 102:9377–81. [PubMed: 15967985]
18. Ozburn AR, Falcon E, Mukherjee S, Gillman A, Arey R, Spencer S, McClung CA. The role of clock in ethanol-related behaviors. Neuropsychopharmacology. 2013; 38:2393–400. [PubMed: 23722243]
19. Ozburn AR, Larson EB, Self DW, McClung CA. Cocaine self-administration behaviors in ClockΔ19 mice. Psychopharmacology (Berl). 2012; 223:169–77. [PubMed: 22535308]
20. Van Enkhuizen J, Minassian A, Young JW. Further evidence for ClockΔ19 mice as a model for bipolar disorder mania using cross-species tests of exploration and sensorimotor gating. Behav Brain Res. 2013; 249:44–54. [PubMed: 23623885]
21. Spencer S, Torres-Altoro MI, Falcon E, Arey R, Marvin M, Goldberg M, et al. A mutation in CLOCK leads to altered dopamine receptor function. J Neurochem. 2012; 123:124–34. [PubMed: 22757753]
22. Coque L, Mukherjee S, Cao J-LL, Spencer S, Marvin M, Falcon E, et al. Specific role of VTA dopamine neuronal firing rates and morphology in the reversal of anxiety-related, but not depression-related behavior in the ClockΔ19 mouse model of mania. Neuropsychopharmacology. 2011; 36:1478–88. [PubMed: 21430648]
23. Carlezon WA, Thomas MJ. Biological substrates of reward and aversion: a nucleus accumbens activity hypothesis. Neuropharmacology. 2009; 56(Suppl 1):122–32. [PubMed: 18675281]
24. Nicola SM, Surmeier J, Malenka RC. Dopaminergic modulation of neuronal excitability in the striatum and nucleus accumbens. Annu Rev Neurosci. 2000; 23:185–215. [PubMed: 10845063]
25. Beurrier C, Malenka RC. Enhanced inhibition of synaptic transmission by dopamine in the nucleus accumbens during behavioral sensitization to cocaine. J Neurosci. 2002; 22:5817–22. [PubMed: 12122043]
26. Russo SJ, Nestler EJ. The brain reward circuitry in mood disorders. Nat Rev Neurosci. 2013; 14:609–25. [PubMed: 23942470]
27. Anand A, Barkay G, Dzemidzic M, Albrecht D, Karne H, Zheng Q-HH, et al. Striatal dopamine transporter availability in unmedicated bipolar disorder. Bipolar Disord. 2011; 13:406–13. [PubMed: 21843280]
28. Dzirasa K, Coque L, Sidor MM, Kumar S, Dancy EA, Takahashi JS, et al. Lithium ameliorates nucleus accumbens phase-signaling dysfunction in a genetic mouse model of mania. J Neurosci. 2010; 30:16314–23. [PubMed: 21123577]
29. Wolf JA, Moyer JT, Lazarewicz MT, Contreras D, Benoit-Marand M, O'Donnell P, Finkel LH. NMDA/AMPA ratio impacts state transitions and entrainment to oscillations in a computational model of the nucleus accumbens medium spiny projection neuron. J Neurosci. 2005; 25:9080–95. [PubMed: 16207867]
30. Castañeda TR, de Prado BM, Prieto D, Mora F. Circadian rhythms of dopamine, glutamate and GABA in the striatum and nucleus accumbens of the awake rat: modulation by light. J Pineal Res. 2004; 36:177–85. [PubMed: 15009508]

31. Boudreau AC, Milovanovic M, Conrad KL, Nelson C, Ferrario CR, Wolf ME. A protein cross-linking assay for measuring cell surface expression of glutamate receptor subunits in the rodent brain after in vivo treatments. Curr Protoc Neurosci Chapter. 2012; 5 Unit 5.30.1-19.
32. Ozburn A, Falcon E, Twaddle A, Nugent A, Gillman A, Spencer S, et al. (n.d.). Direct Regulation of Diurnal Drd3 Expression and Cocaine Reward by NPAS2. Biological Psychiatry.
33. Udagawa T, Fujioka Y, Tanaka M, Honda D, Yokoi S, Riku Y, et al. FUS regulates AMPA receptor function and FTLD/ALS-associated behaviour via GluA1 mRNA stabilization. Nat Commun. 2015; 6:7098. [PubMed: 25968143]
34. Mukherjee S, Coque L, Cao J-LL, Kumar J, Chakravarty S, Asaithamby A, et al. Knockdown of Clock in the ventral tegmental area through RNA interference results in a mixed state of mania and depression-like behavior. Biol Psychiatry. 2010; 68:503–11. [PubMed: 20591414]
35. Faure A, Richard JM, Berridge KC. Desire and dread from the nucleus accumbens: cortical glutamate and subcortical GABA differentially generate motivation and hedonic impact in the rat. PLoS ONE. 2010; 5:e11223. [PubMed: 20585461]
36. Meredith GE, Baldo BA, Andrezjewski ME, Kelley AE. The structural basis for mapping behavior onto the ventral striatum and its subdivisions. Brain Struct Funct. 2008; 213:17–27. [PubMed: 18256852]
37. Wickens JR, Wilson CJ. Regulation of action-potential firing in spiny neurons of the rat neostriatum in vivo. J Neurophysiol. 1998; 79:2358–64. [PubMed: 9582211]
38. Vilchis C, Bargas J, Ayala GX, Galván E, Galarraga E. Ca2+ channels that activate Ca2+-dependent K+ currents in neostriatal neurons. Neuroscience. 2000; 95:745–52. [PubMed: 10670441]
39. Shen W, Hernandez-Lopez S, Tkatch T, Held JE, Surmeier DJ. Kv1.2-containing K+ channels regulate subthreshold excitability of striatal medium spiny neurons. J Neurophysiol. 2004; 91:1337–49. [PubMed: 13679409]
40. Sidor MM, Spencer SM, Dzirasa K, Parekh PK, Tye KM, Warden MR, et al. Daytime spikes in dopaminergic activity drive rapid mood-cycling in mice. Mol Psychiatry. 2015; 20:1406–19. [PubMed: 25560763]
41. Boudreau AC, Wolf ME. Behavioral sensitization to cocaine is associated with increased AMPA receptor surface expression in the nucleus accumbens. J Neurosci. 2005; 25:9144–51. [PubMed: 16207873]
42. Conrad KL, Tseng KY, Uejima JL, Reimers JM, Heng L-JJ, Shaham Y, et al. Formation of accumbens GluR2-lacking AMPA receptors mediates incubation of cocaine craving. Nature. 2008; 454:118–21. [PubMed: 18500330]
43. Lüscher C, Malenka RC. Drug-evoked synaptic plasticity in addiction: from molecular changes to circuit remodeling. Neuron. 2011; 69:650–63. [PubMed: 21338877]
44. Mu P, Moyer JT, Ishikawa M, Zhang Y, Panksepp J, Sorg BA, et al. Exposure to cocaine dynamically regulates the intrinsic membrane excitability of nucleus accumbens neurons. J Neurosci. 2010; 30:3689–99. [PubMed: 20220002]
45. Moyer JT, Wolf JA, Finkel LH. Effects of dopaminergic modulation on the integrative properties of the ventral striatal medium spiny neuron. J Neurophysiol. 2007; 98:3731–48. [PubMed: 17913980]
46. Kolaj M, Zhang L, Rønnekleiv OK, Renaud LP. Midline thalamic paraventricular nucleus neurons display diurnal variation in resting membrane potentials, conductances, and firing patterns in vitro. J Neurophysiol. 2012; 107:1835–44. [PubMed: 22219029]
47. Malkoff-Schwartz S, Frank E, Anderson BP, Hlastala SA, Luther JF, Sherrill JT, et al. Social rhythm disruption and stressful life events in the onset of bipolar and unipolar episodes. Psychol Med. 2000; 30:1005–16. [PubMed: 12027038]
48. Grandin LD, Alloy LB, Abramson LY. The social zeitgeber theory, circadian rhythms, and mood disorders: review and evaluation. Clin Psychol Rev. 2006; 26:679–94. [PubMed: 16904251]
49. Levenson JC, Wallace ML, Anderson BP, Kupfer DJ, Frank E. Social rhythm disrupting events increase the risk of recurrence among individuals with bipolar disorder. Bipolar Disord. 2015; 17:869–79. [PubMed: 26614534]

50. Wiedholz LM, Owens WA, Horton RE, Feyder M, Karlsson R-MM, Hefner K, et al. Mice lacking the AMPA GluR1 receptor exhibit striatal hyperdopaminergia and “schizophrenia-related” behaviors. Mol Psychiatry. 2008; 13:631–40. [PubMed: 17684498]

51. Boyce-Rustay JM, Holmes A. Genetic inactivation of the NMDA receptor NR2A subunit has anxiolytic- and antidepressant-like effects in mice. Neuropsychopharmacology. 2006; 31:2405–14. [PubMed: 16482087]

52. Shaltiel G, Maeng S, Malkesman O, Pearson B, Schloesser RJ, Tragon T, et al. Evidence for the involvement of the kainate receptor subunit GluR6 (GRIK2) in mediating behavioral displays related to behavioral symptoms of mania. Mol Psychiatry. 2008; 13:858–72. [PubMed: 18332879]

53. Bachtell RK, Choi K-HH, Simmons DL, Falcon E, Monteggia LM, Neve RL, Self DW. Role of GluR1 expression in nucleus accumbens neurons in cocaine sensitization and cocaine-seeking behavior. Eur J Neurosci. 2008; 27:2229–40. [PubMed: 18430032]

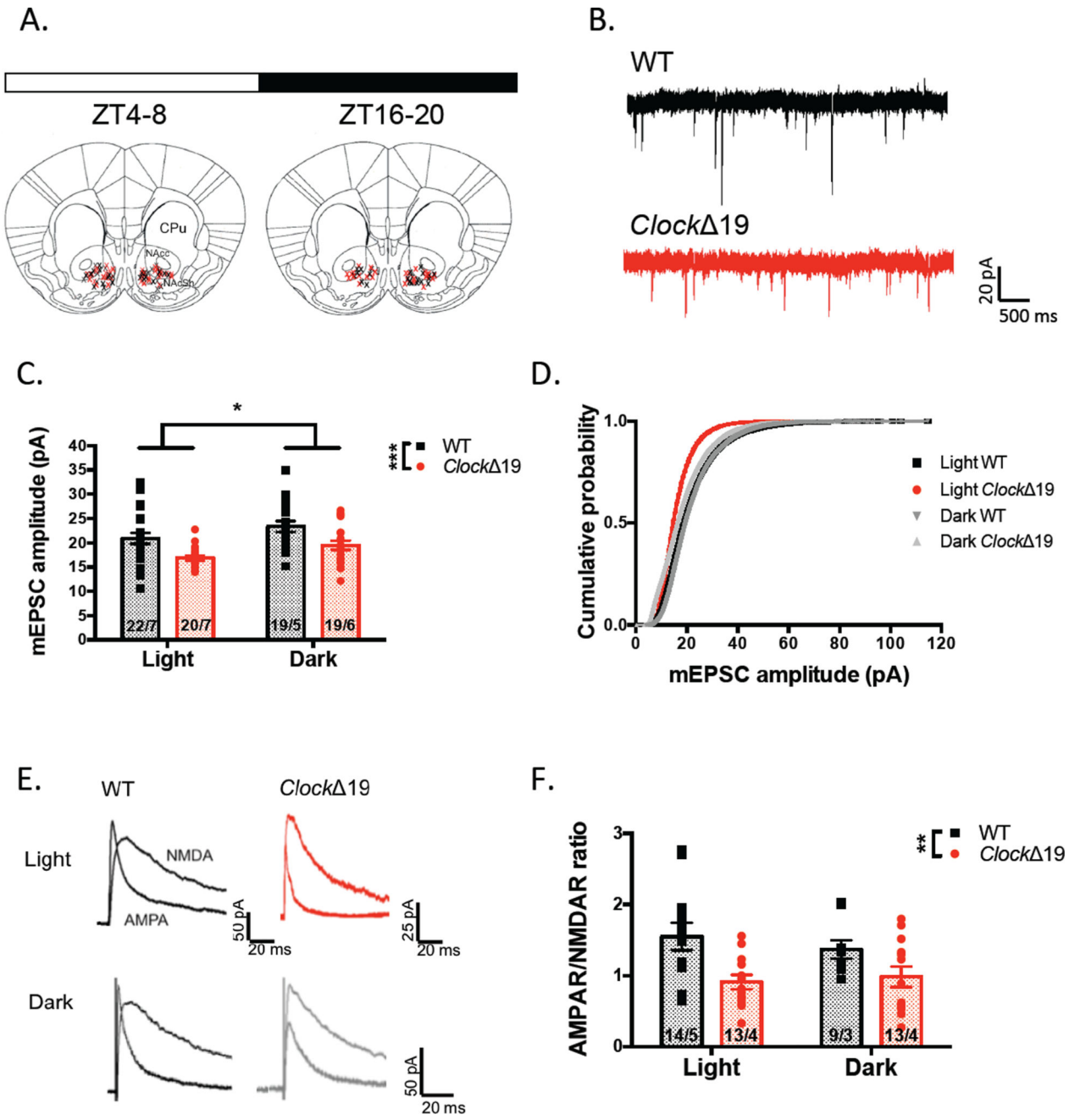

Figure 1.

*Clock*Δ19 mutation modifies MSN AMPAR-mediated synaptic transmission and strength. (A) Recording sites within the NAc from slices collected during light and dark phases (WT – black; *Clock*Δ19 – red; ZT = Zeitgeber time; CPu = caudate putamen; NAcc = NAc core; NAcSh = NAc shell). (B) Representative traces of mEPSCs recorded at −70mV in the presence of 1uM TTX. (C) Summary of mEPSC amplitude of mutant and WT MSNs at both phases (n = cells/animals; all data in bar graphs are presented as mean ± SEM). (D) Plot of cumulative probability of all mEPSC amplitudes across phases. (E) Representative traces of evoked AMPAR and NMDAR-mediated EPSCs at 40mV. (F) Ratio of the peak amplitude of

the AMPAR EPSC to the NMDAR EPSC for each group of MSNs. *$P < 0.05$; **$P < 0.01$; ***$P < 0.001$ in this and all subsequent figures.

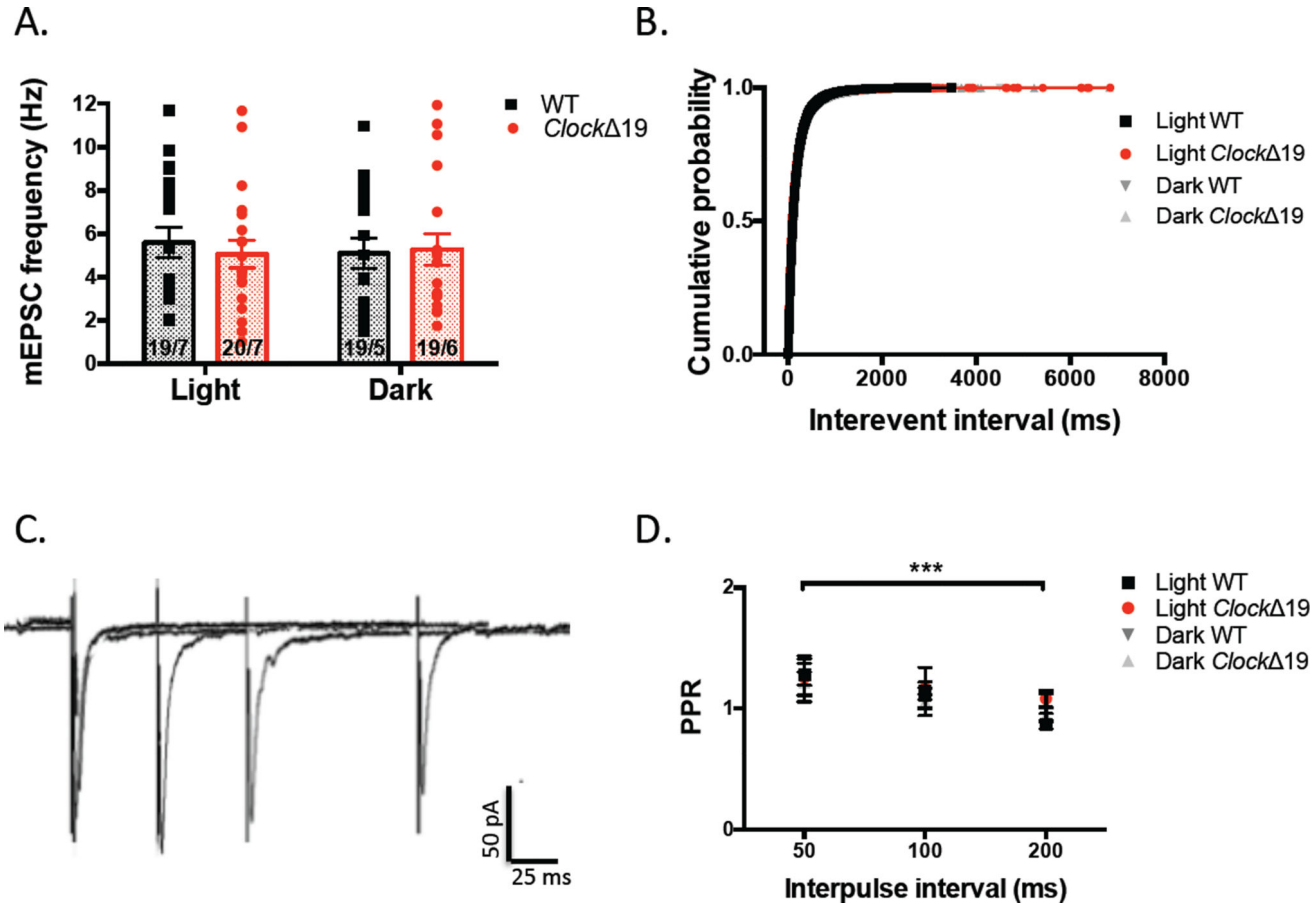

Figure 2.

*Clock*Δ19 mutation does not alter the presynaptic function of NAc MSNs. (A) Frequency of AMPAR mEPSCs recorded from mutant and WT MSNs at light and dark phases. (B) Cumulative probability of inter-event intervals (IEI) of all recorded mEPSCs. (C) Sample traces of pairs of evoked AMPAR EPSCs at −70mV at varying inter-stimulus intervals. (D) Paired-pulse ratio (PPR) calculated as peak amplitude of the second EPSC to the first plotted across inter-stimulus interval.

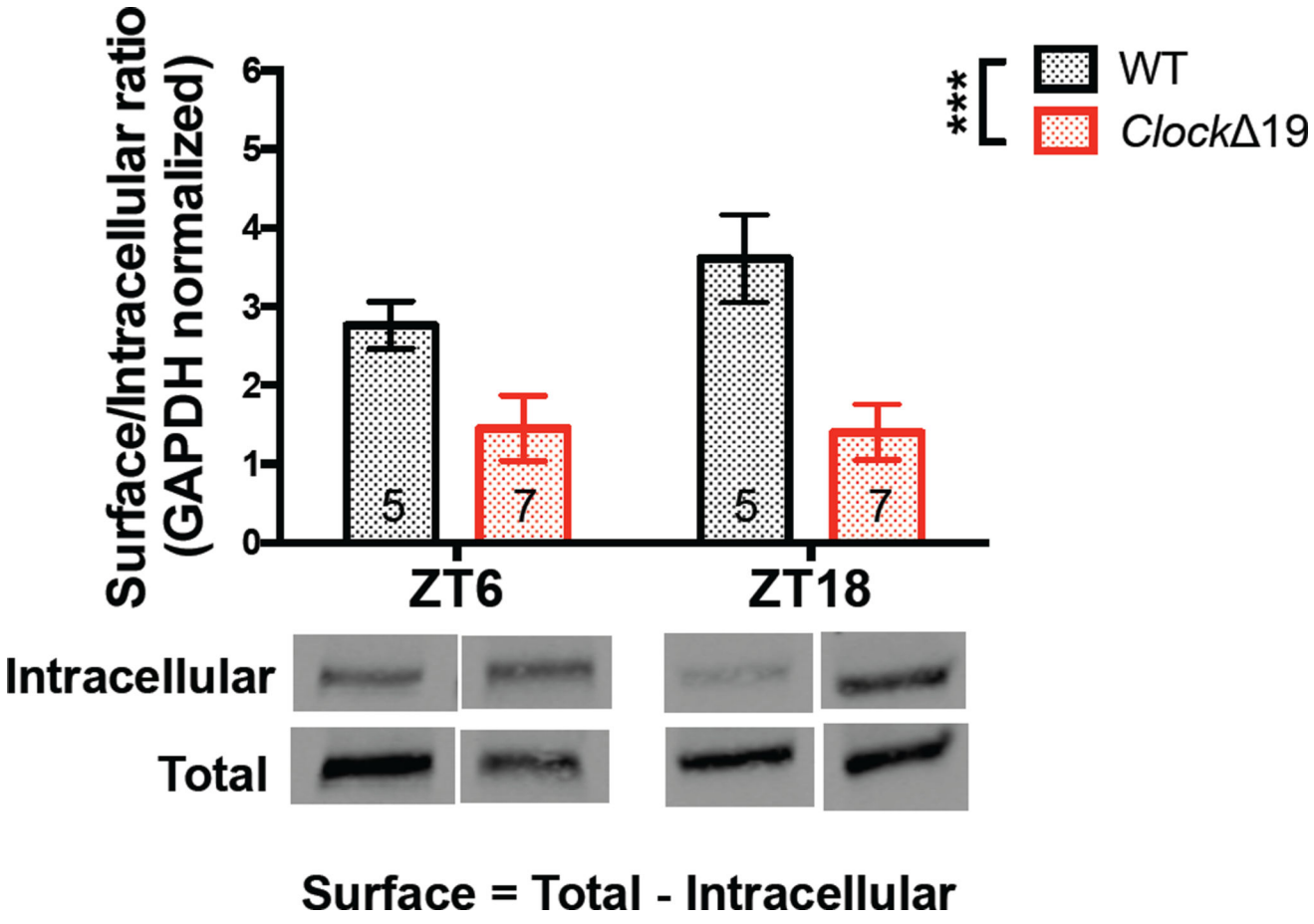

Figure 3.

The surface/intracellular ratio of GLUA1 expression is significantly reduced in *Clock*Δ19 NAc during the light (ZT6) and dark (ZT18) phases. Crosslinked and non-crosslinked NAc tissue from mutant and WT animals allowed for the quantification of total and intracellular protein levels of GLUA1. Surface protein levels were inferred by the subtraction of intracellular protein from total protein. *Clock*Δ19 mice have significantly reduced S/I ratio of GLUA1 compared with WT littermates at ZT6 and ZT18. Representative bands are shown below. Band intensity was normalized to GAPDH and presented as arbitrary units (n = 5–7 mice for all groups).

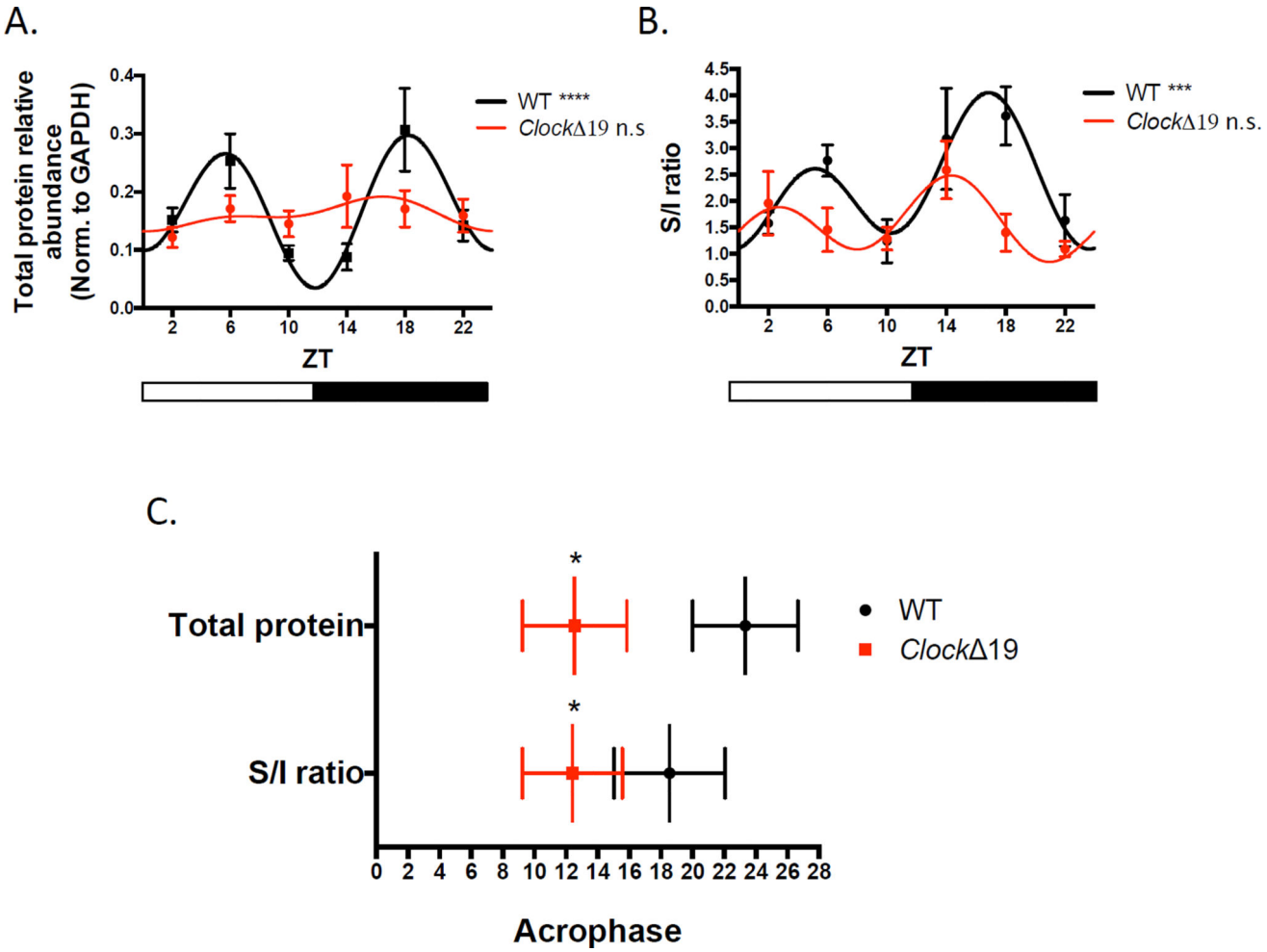

Figure 4.

A diurnal rhythm in GLUA1 expression in WT mice is abolished in *Clock* mutants. (A) The diurnal rhythm of total protein levels of GLUA1 across 6 time points, normalized to GAPDH expression in mutant and WT NAc tissue. A significant curve fit was found in WT but not in mutant data (bars below represent light and dark phases). (B) Rhythmic profile of the GLUA1 S/I ratio in WT and mutant across the light/dark cycle showing a loss of significant rhythm in mutant NAc. (C) Acrophase of diurnal expression rhythms of total GLUA1 and S/I ratio in mutant and WT accumbens. Acrophase measures were derived from the center of gravity of the fitted harmonic curves (+SEM; $n = 5–9$ mice for all groups).

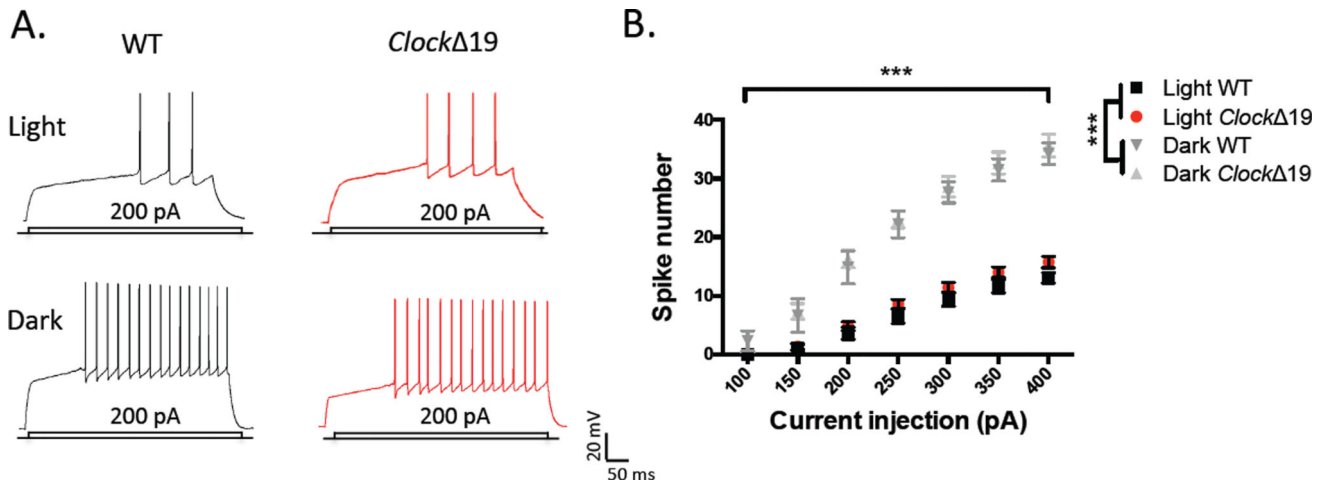

Figure 5.

Excitability of MSNs is unaltered by *Clock*Δ19 mutation however diurnal variation exists in evoked firing rates of NAc MSNs. (A) Representative traces of action potential firing in response to current injection from mutant and WT MSNs during the light and dark phases. (B) Input-output curve of spikes with varying current steps during both phases in both groups.

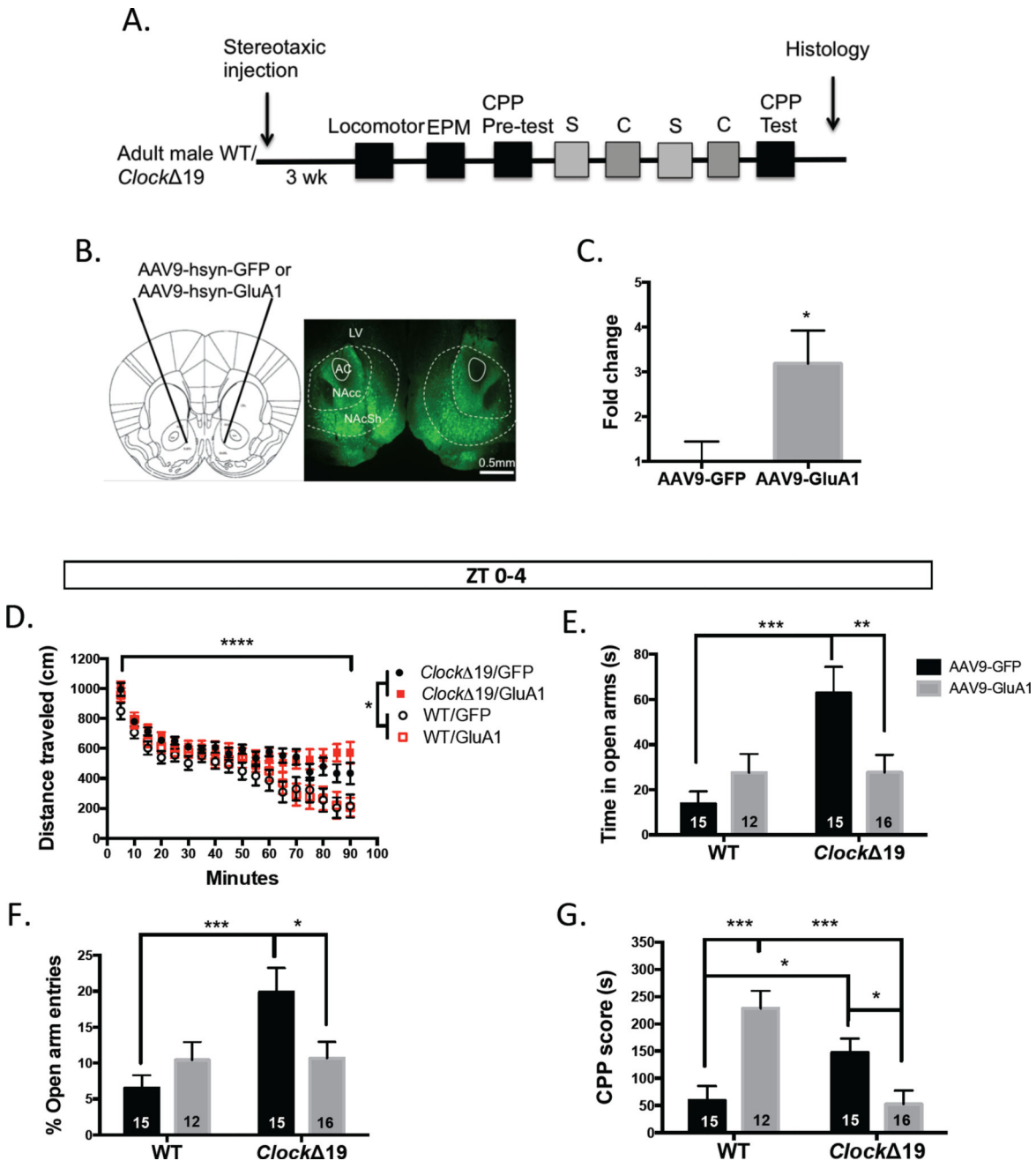

Figure 6.

Functional up-regulation of *GluA1* in the NAc of *Clock*Δ19 mice normalizes exploratory drive behavior and conditioned reward sensitivity during the light phase. (A) Timeline of experimental procedures testing the effect of AAV9-hsyn-*GluA1* or AAV9-hsyn-GFP expression on behavior in mutant and WT mice (S – saline; C – cocaine) (B) Representative image of GFP viral expression localized to the NAc. (C) Accumbal *GluA1* transcript levels following viral overexpression compared with GFP expression. (D) Locomotor activity in a novel environment of mutant and WT animals. (E) Total time spent in the open arms of the EPM during 10 min of testing. (F) Percent open arm entries in the EPM normalized to total

crosses. (G) Cocaine CPP scores of all experimental groups following a biased conditioning paradigm. LV- lateral ventricle; AC – anterior commissure; NAcc – nucleus accumbens core; NAcSh – nucleus accumbens shell.

Table 1

Intrinsic membrane properties of *Clock* mutant and WT MSNs during light and dark phases. Additional properties of membrane excitability of MSNs were examined in *Clock*Δ19 and WT cells including resting membrane potential at break-in, (RMP), rheobase, action potential (AP) threshold and input resistance (R_i).

Light phase MSN membrane properties			
Genotype	**Wildtype**	***Clock* mutant**	***p*-value**
Number of cells	*n* = 14/6	*n* = 15/4	
Break-in RMP (mV)	−80.50 ± 1.92	−85.33 ± 1.09	**0.0352***
Rheobase (pA)	185.7 ± 15.22	176.7 ± 10.76	0.62760
AP threshold (mV)	−32.83 ± 2.53	−35.35 ± 1.29	0.37940
Input resistance (MΩ)	166.6 ± 12.39	204.6 ± 14.37	0.06320
Dark phase MSN membrane properties			
Number of cells	*n* = 7/5	*n* = 9/4	
Break-in RMP (mV)	−83.71 ± 1.55	−88.11 ± 0.73	**0.0155***
Rheobase (pA)	137.5 ± 18.30	127.8 ± 8.78	0.62640
AP threshold (mV)	−34.80 ± 3.24	−42.29 ± 1.36	**0.0358***
Input resistance (MΩ)	183.5 ± 26.39	225.7 ± 27.29	0.29040